CHINESE OPTICS LETTERS

Vol. 21, No. 8 | August 2023

Coherent combining of a fiber laser array via cascaded internal phase control technique

Jinhu Long (龙金虎)[1], Jiayi Zhang (张嘉怡)[1], Hongxiang Chang (常洪祥)[1], Qi Chang (常 琦)[1], Yu Deng (邓 宇)[1], Zixin Yang (杨子鑫)[1], Jian Wu (吴 坚)[1], Rongtao Su (粟荣涛)[1,2*], Yanxing Ma (马阎星)[1,2], Pengfei Ma (马鹏飞)[1,2], and Pu Zhou (周 朴)[1**]

[1] College of Advanced Interdisciplinary Studies, National University of Defense Technology, Changsha 410073, China

[2] Nanhu Laser Laboratory, National University of Defense Technology, Changsha 410073, China

*Corresponding author: surongtao@126.com

**Corresponding author: zhoupu203@163.com

Received January 2, 2023 | Accepted April 25, 2023 | Posted Online August 7, 2023

We experimentally demonstrated a cascaded internal phase control technique. A laser array with 12 channels was divided into three sub-arrays and a stage array, and phases of the sub-arrays and the stage array were locked by four phase controllers based on the stochastic parallel gradient descent (SPGD) algorithm, respectively. In this way, the phases of the whole array were locked, and the visibility of the interference pattern of the whole emitted laser array in the far field was ~93%. In addition, the technique has the advantage of element expanding and can be further used in the high-power coherent beam combination (CBC) system due to its compact spatial structure.

Keywords: coherent beam combining; laser array; cascaded control; internal phase control.

DOI: 10.3788/COL202321.081402

1. Introduction

High-power fiber laser is always attracting attention due to its fascinating properties, including high efficiency and excellent beam quality[1,2], which has promoted various of applications, such as interferometric gravitational wave detecting[3,4] and industrial processing[1]. However, the power scaling capacity of a monolithic fiber laser remains a critical challenge due to physical limitations, such as nonlinear effects and fiber damage[5–8]. Addressing the challenge, the coherent beam combining (CBC) technique provides an available solution, which can break through the output power limitations while maintaining high beam quality[9–12]. To date, the CBC technique has presented an impressive performance with the combined number of being 100 elements[13-15] and the output power being over 10 kW[16–18].

In a CBC system, it is critically important to lock the phases of the beamlets, meaning that one needs to detect the phases and send the feedback optical signals to the phase control system. Up to now, many available techniques have been put forward and demonstrated in the experiment, such as the stochastic parallel gradient descent (SPGD) algorithm[13,18–21], dithering technique[22–25], and interference measurement[15,26,27]. Moreover, the new techniques, including machine learning[28,29], adaptive space-to-fiber laser beam coupling[30], the square wave dithering algorithm[31], and the self-imaging effect method[32], also exhibit the impressive performances for phase locking in the CBC system. However, the additional power scaling and elements expanding of these methods face two challenges. First, these techniques detect the phases of the beamlets after they are combined and emitted to the free space, which are always called external phase control technique[33–35]. When the apertures of the beamlets are expanded to obtain the high fill-factor, the emitted laser array always has a large cross section, which needs large aperture optical devices to sample the beams, such as the lens and beam splitters. The large optical devices would rise a difficulty in phase control[34,36]. Moreover, the control bandwidth would decrease when increasing the number of the beamlets, which can cause the failure of phase locking and decrease the combination efficiency[13,34]. Therefore, to solve the problems, the internal phase control technique can help us to avoid the large aperture optical devices and make the phase control system compact[33–35]. Meanwhile, the cascaded phase control technique can be applied to improve the control bandwidth[37,38].

In this Letter, a cascaded internal phase control technique was demonstrated by the experiment. An experimental setup with a 12-channel laser array was built. In the experiment, the laser array was divided into three sub-arrays and a stage array. When the phases of each sub-array were locked by the SPGD algorithm, the phase differences of the emitted laser array were

compensated effectively. The visibility of the interference pattern of the whole emitted laser array in the far field was ~93%, which meant that the CBC of a massive laser array with the cascaded internal phase control technique was feasible. Owing to the compact spatial structure, the technique can be used in the high-power CBC system. This work could offer an available reference for the phase control of a massive laser array.

2. Experimental Setup

Figure 1 shows the experimental setup. The seed laser (SL) is a single-clad ytterbium-doped polarization-maintained single-frequency fiber laser with a core diameter of 6 μm and a cladding diameter of 125 μm. The central wavelength is 1064 nm, while the linewidth is 20 kHz and the output power is 30 mW. The laser power from the SL is pre-amplified to 500 mW by a pre-amplifier (PA) and split into three channels to form three laser sub-arrays using a fiber splitter (FS), where each sub-array has four beamlets. To simplify the schematic diagram, we only drew two beamlets in each sub-array, as shown in Fig. 1. In each sub-array, the laser is coupled into the first stage $LiNbO_3$ phase modulator (1st-PM) and the PA to amplify the power to 500 mW. Then, the laser is coupled into the FS and split into four channels to form a sub-array. After that, in each sub-array, three channels are coupled with the second stage $LiNbO_3$ phase modulators (2nd-PM), while another channel is not coupled with the 2nd-PM, which can be used for cascaded phase control[38]. The response frequency of the $LiNbO_3$ phase modulator is about 150 MHz, which is operating on 1064 nm. Following that, all the laser channels transmit to the cascaded fiber amplifier (CFA) to amplify the power to 500 mW. Lastly, all the beamlets are collimated using the collimators (CO) and transmitted to the free space. The diameter of each collimated beamlet is about 10 mm, while the distance among the adjacent beamlets is about 40 mm.

To avoid the large aperture optical devices, all the collimated beamlets are sampled by a small beam splitter (SP) array. More than 99% laser power is reflected to the laser emitting system to form the emitted laser array, while less than 1% laser power

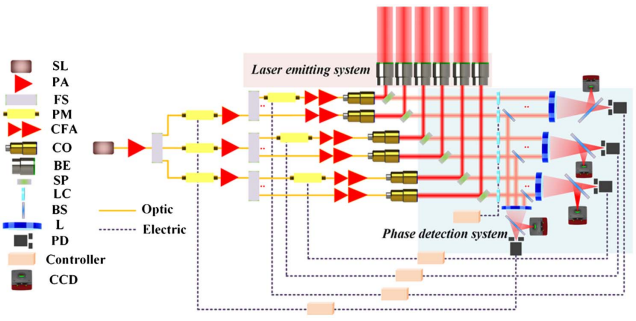

Fig. 1. Experimental setup of the internal phase sensing system. SL, seed laser; PA, pre-amplifier; FS, fiber splitter; PM, phase modulator; CFA, cascaded fiber amplifier; CO, collimator; BE, beam expander; SP, small beam splitter; LC, liquid crystal; BS, beam splitter; L, lens; PD, photodetector.

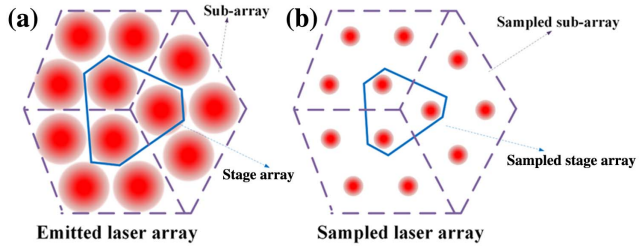

Fig. 2. Schematic drawing of the laser array. (a) The emitted laser array and (b) the corresponding sampled laser array.

transmits the phase detection system to form the sampled laser array. In the emitted laser array, each beamlet is expanded by the beam expander (BE) to obtain the high fill-factor of ~95%, and the diameter of each expanded beamlet is about 38 mm, as shown in Fig. 2(a). In terms of phase control, all the beamlets transmit the liquid crystals (LCs) and then are divided into three sampled sub-arrays. The LC is used for compensating the external phase differences[34], and the diameter of the LC is 20 mm. Subsequently, the beamlets in the adjacent sampled sub-arrays are reflected by the beam splitters (BS) and combined to form the sampled stage array, as shown in Fig. 2(b), which is circled with solid blue lines. These beamlets are not coupled with the 2nd-PMs, while the other beamlets are all coupled with the 2nd-PMs. The reflectivity of the BS is 50%. Lastly, each sampled sub-array is focused by a lens (L) with a focal length of 1 m, while the sampled stage array is focused by an L with a focal length of 500 mm. To observe the combined beams in each sampled sub-array and stage array, several beam splitters (BS) with a reflectivity of 50% are set in the optical paths and split the combined beams into two parts. One part is observed by a charge-coupled device (CCD) camera, which is positioned at the focal plane of the L in each sampled sub-array. Another part is detected by a Si photodetector (PD), which is operating on 350–1100 nm, and a pinhole with a diameter of 50 μm is set in front of each PD to truncate the power in the bucket (PIB) of the combined beams. The signals from the PDs are sent to the controllers to control the PMs. In the experiment, all the controllers are performed using the SPGD algorithm.

3. Experimental Results and Discussion

The process of phase locking in each sub-array could be observed by the PIB values in the PDs, as shown in Fig. 3. When the phase control system was in the open loop, all the PIB values changed randomly along the time because of the dynamic phase noises. The normalized average values were around 0.15, 0.21, 0.38, and 0.63, respectively. As a contrast, when all the controllers were turned on and performed using the SPGD algorithm continuously, PIB values were stably locked to be the maximums. The normalized average values were 0.95, 0.92, 0.93, and 0.91, respectively. Thus, the internal phase noises among the sampled laser array were locked to be 0 or $2n\pi$, where n was an integer. In addition, the corresponding root mean

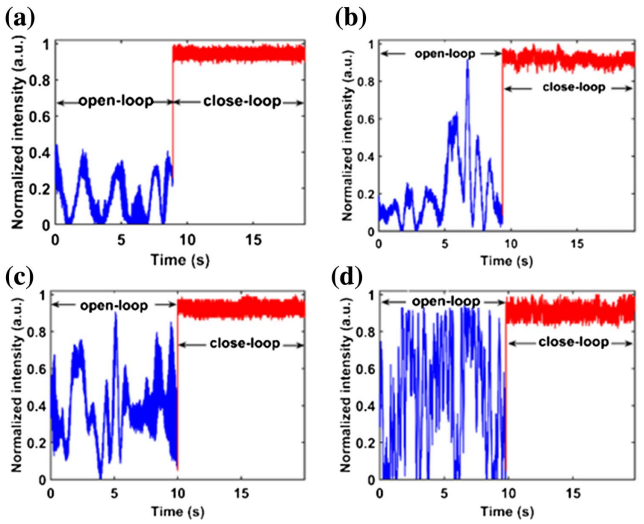

Fig. 3. The PIB of the combined beams detected by the PDs in the open and closed loops. (a) Sampled sub-array 1, (b) sampled sub-array 2, (c) sampled sub-array 3, and (d) sampled stage array.

square (RMS) of the residual phase error of each sub-array was calculated to be $\lambda/27$, $\lambda/23$, $\lambda/22$, and $\lambda/20$, respectively.

Figure 4 shows the irradiance distribution of each sampled sub-array during the phase-locking process. One can see that when all the controllers were turned off, the irradiance distribution of the combined beams had low contrast, and the brightness was weak, as shown in Figs. 4(a1)–4(d1). In comparison, when all the controllers were turned on, the phases of the sampled beamlets could be locked to be the same value. As a result, the irradiance distributions of each sampled sub-array and stage array were locked stably, as shown in Figs. 4(a2)–4(d2). The energy of the irradiance distribution was concentrated in the central lobe, and the visibilities of the interference patterns in the far field were 98%, 97%, 96%, and 89%, respectively. The visibility of the interference patterns was defined as $(I_{\max} - I_{\min})/(I_{\max} + I_{\min})$, where $I_{\max}$ and $I_{\min}$ were the maximum light intensity and the adjacent minimum light intensity of the interference pattern, respectively. Therefore, one can

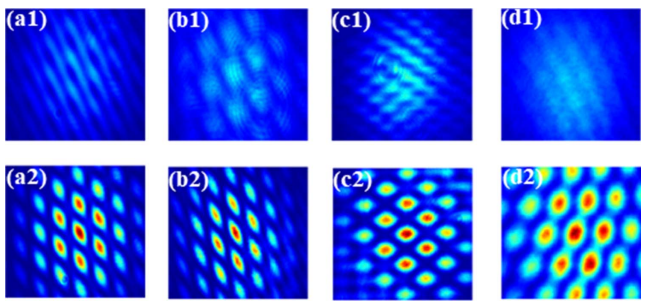

Fig. 4. The irradiance distributions of the (a1) sampled sub-array 1, (b1) sampled sub-array 2, (c1) sampled sub-array 3, and (d1) sampled stage array when all the controllers are turned off. The irradiance distributions of the (a2) sampled sub-array 1, (b2) sampled sub-array 2, (c2) sampled sub-array 3, and (d2) sampled stage array when all the controllers are turned on.

conclude that the sampled laser array can be locked with the same phase wavefront based on the cascaded internal phase control.

Here, the internal dynamic phase noises were locked. However, there are some external phase differences among the beamlets in the emitted laser array due to the different optical paths[34]. Fortunately, the external phase differences are generally static and can be compensated by the interference methods[15,27]. In our experiment, a large aperture lens (L2) was applied to focus the emitted laser array to form a far field. The focus length of the L2 was 2 m, and the combined beams in the far field were observed by a CCD, as shown in Fig. 5. In the experiment, the external phase differences in each emitting sub-array and stage array were detected and compensated by the LCs independently according to the method in Ref. [34], respectively.

The irradiance distributions of the emitted sub-arrays and stage array are shown in Fig. 6. When all the controllers were turned off, all the combined beams in the far field had weak brightness with low contrast, as shown in Figs. 6(a1)–6(d1), while the brightness was effectively promoted when all the

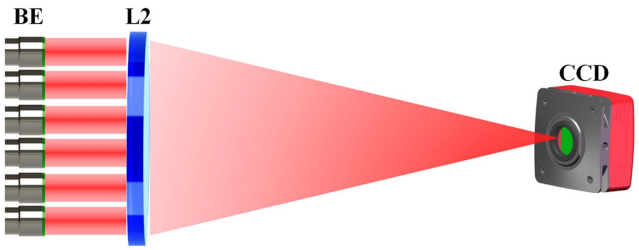

Fig. 5. Experimental setup for observing the combined beams in the emitting laser array. BE, beam expander; L, lens; CCD, CCD camera).

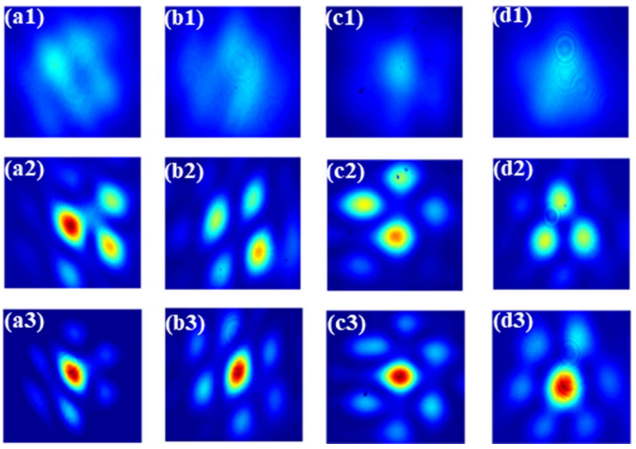

Fig. 6. The irradiance distributions (IDs) of the (a1) sub-array 1, (b1) sub-array 2, (c1) sub-array 3, and (d1) stage array when all the controllers are turned off. The IDs of the (a2) sub-array 1, (b2) sub-array 2, (c2) sub-array 3, and (d2) stage array when all the controllers are turned on. The IDs of the (a3) sub-array 1, (b3) sub-array 2, (c3) sub-array 3, and (d3) stage array after external phase difference compensation.

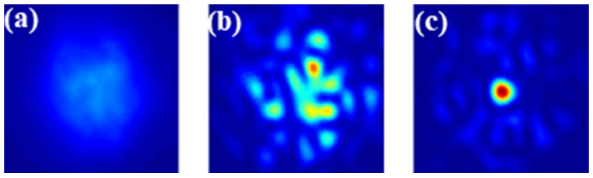

Fig. 7. The irradiance distribution of the whole emitting laser array detected by CCD when (a) all the controllers are turned off and (b) turned on without external phase difference compensation. (c) After external phase difference compensation.

controllers were turned on, as shown in Figs. 6(a2)–6(d2). However, the irradiance distribution was not concentrated in the central lobe due to the external phase differences. When the external phase differences were compensated, all the brightness of the irradiance distribution was promoted to be the maximum, as shown in Figs. 6(a3)–6(d3). The visibility of the interference pattern in each sub-array was 94%, 94%, 93%, and 91%, respectively.

At last, the whole emitted laser array is detected by the CCD. The irradiance distribution of the whole emitted laser array is shown in Fig. 7. One can find that the brightness of irradiance distribution was promoted effectively after external phase difference compensation. The visibility of the interference patterns in the far field was 93%. That meant the phases of all the emitted beamlets had been locked to be the same value. In addition, the PIB was calculated to be ~42%, which was 50% in an ideal CBC system. Thus, the CBC efficiency was ~84%. The PIB loss may be caused by the residual phase error and the tilt phase error[13]. To further improve the CBC efficiency, the residual phase error could be decreased by optimizing the control parameters of the phase control system. Meanwhile, the adaptive fiber-optics collimator (AFOC) or a fast piezo steering mirror (FPSM) could be used for decreasing the tilt phase error[30].

Based on the preliminary experiment, the feasibility of CBC of a massive laser array by the cascaded internal phase control has been verified. In the experiment, in each sampled sub-array, a BS with a reflectivity of 50% was used to reflect one beamlet to form the sampled stage array, which could cause the power loss of the corresponding beamlet in the sampled sub-array and influence the phase control. Hence, to improve the phase control performance, the reflectivity of the BS should be small enough to balance the output power of each sampled beamlet. To further scale the output power, one can address the problem with two methods. On the one hand, the output power of each laser channel needs to be improved. The linewidth of each laser channel should be broadened to suppress the stimulated Brillouin scattering (SBS) effect[7], and the output power can be further scaled to several kilowatt[7,39,40]. On the other hand, the combined elements should be further expanded. One can increase the number of the sub-arrays and the number of the beamlets in each sub-array, which were analyzed in Ref. [38]. Recently, the efficient phase locking of nineteen kilowatt-level narrow linewidth fiber amplifiers has been realized in the experiment[18]. Considering the power scaling capacity of each laser channel and the expanding capacity of the beam elements, our technique can be further used in the high-power CBC system for obtaining the high-power laser.

4. Conclusion

In conclusion, we experimentally demonstrated a cascaded internal phase control technique with a 12-channel laser array. In the experiment, the whole laser array was divided into three sub-arrays and a stage array. The detailed results indicated that when all the controllers were performed using the SPGD algorithm, the phases of each sub-array could be locked. The normalized average values of the PIB were 0.95, 0.92, 0.93, and 0.91, respectively. The corresponding RMS of phase deviations were less than $\lambda/27$, $\lambda/23$, $\lambda/22$, and $\lambda/20$, respectively. As a result, the visibility of the interference pattern of the whole laser array in the far field was ~93%, which meant that the CBC of a massive laser array by the cascaded internal phase control was feasible. In addition, the technique can be further used in the high-power CBC system due to its compact spatial structure. Furthermore, the phase control system is detached from the emitting laser system, and one can freely expand the aperture of the emitted beamlets, which can be beneficial for various applications, such as laser communications and energy transmission. This work could offer a promising solution for the phase control of a massive laser array.

Acknowledgement

This work was supported by the National Natural Science Foundation of China (Nos. 62275272 and 62075242), the Natural Science Foundation of Hunan Province, China (No. 2019JJ10005), the Training Program for Excellent Young Innovators of Changsha (No. kq2206003), and the Postgraduate Scientific Research Innovation Project of Hunan Province (No. QL20220013).

References

1. C. Jauregui, J. Limpert, and A. Tünnermann, "High-power fibre lasers," Nat. Photonics **7**, 861 (2013).
2. C. N. Danson, C. Haefner, and J. Bromage, et al., "Petawatt and exawatt class lasers worldwide," High Power Laser Sci. Eng. **7**, e54 (2019).
3. C. Robin, I. Dajani, and B. Pulford, "Modal instability-suppressing, single-frequency photonic crystal fiber amplifier with 811 W output power," Opt. Lett. **39**, 666 (2014).
4. J. Zhao, G. Guiraud, C. Pierre, F. Floissat, A. Casanova, A. Hreibi, W. Chaibi, N. Traynor, J. Boullet, and G. Santarelli, "High-power all-fiber ultra-low noise laser," Appl. Phys. B **124**, 114 (2018).
5. J. W. Dawson, M. J. Messerly, R. J. Beach, M. Y. Shverdin, E. A. Stappaerts, A. K. Sridharan, P. H. Pax, J. E. Heebner, C. W. Siders, and C. P. J. Barty, "Analysis of the scalability of diffraction-limited fiber lasers and amplifiers to high average power," Opt. Express **16**, 13240 (2008).
6. C. Stihler, C. Jauregui, S. E. Kholaif, and J. Limpert, "Intensity noise as a driver for transverse mode instability in fiber amplifiers," PhotoniX **1**, 8 (2020).
7. Z.-M. Huang, Q. Shu, R.-M. Tao, Q.-H. Chu, Y. Luo, D.-L. Yan, X. Feng, Y. Liu, W.-J. Wu, H.-H. Zhang, H. Lin, J.-J. Wang, and F. Jing, ">5 kW

record high power narrow linewidth laser from traditional step-index monolithic fiber amplifier," IEEE Photon. Technol. Lett. **33**, C1 (2021).
8. S. Ren, W. Lai, G. Wang, W. Li, J. Song, Y. Chen, P. Ma, W. Liu, and P. Zhou, "Experimental study on the impact of signal bandwidth on the transverse mode instability threshold of fiber amplifiers," Opt. Express **30**, 7845 (2022).
9. T. Y. Fan, "Laser beam combining for high-power, high-radiance sources," IEEE J. Sel. Top. Quantum Electron. **11**, 567 (2005).
10. A. Brignon, ed., *Coherent Laser Beam Combining* (Wiley-VCH, 2013).
11. R. Liu, C. Peng, W. Wu, X. Liang, and R. Li, "Coherent beam combination of multiple beams based on near-field angle modulation," Opt. Express **26**, 2045 (2018).
12. Z. Liu, X. Jin, R. Su, P. Ma, and P. Zhou, "Development status of high power fiber lasers and their coherent beam combination," Sci. China Inf. Sci. **62**, 41301 (2019).
13. H. Chang, Q. Chang, J. Xi, T. Hou, R. Su, P. Ma, J. Wu, C. Li, M. Jiang, Y. Ma, and P. Zhou, "First experimental demonstration of coherent beam combining of more than 100 beams," Photonics Res. **8**, 1943 (2020).
14. M. Shpakovych, G. Maulion, V. Kermene, A. Boju, P. Armand, A. Desfarges-Berthelemot, and A. Barthélemy, "Experimental phase control of a 100 laser beam array with quasi-reinforcement learning of a neural network in an error reduction loop," Opt. Express **29**, 12307 (2021).
15. Q. Chang, T. Hou, J. Long, Y. Deng, H. Chang, P. Ma, R. Su, Y. Ma, and P. Zhou, "Experimental phase stabilization of a 397-channel laser beam array via image processing in dynamic noise environment," J. Lightwave Technol. **40**, 6542 (2022).
16. E. Shekel, Y. Vidne, and B. Urbach, "16 kW single mode CW laser with dynamic beam for material processing," Proc. SPIE **11260**, 1126021 (2020).
17. M. Müller, C. Aleshire, A. Klenke, E. Haddad, F. Légaré, A. Tünnermann, and J. Limpert, "10.4 kW coherently combined ultrafast fiber laser," Opt. Lett. **45**, 3083 (2020).
18. M. Yanxing and P. Ma, "Coherently combined fiber laser with 20 kW high power output," Infrared Laser Eng. **50**, 20210621 (2021).
19. C. X. Yu, S. J. Augst, S. M. Redmond, K. C. Goldizen, D. V. Murphy, A. Sanchez, and T. Y. Fan, "Coherent combining of a 4 kW, eight-element fiber amplifier array," Opt. Lett. **36**, 2686 (2011).
20. C. Geng, W. Luo, Y. Tan, H. Liu, J. Mu, and X. Li, "Experimental demonstration of using divergence cost-function in SPGD algorithm for coherent beam combining with tip/tilt control," Opt. Express **21**, 25045 (2013).
21. T. Weyrauch, M. Vorontsov, J. Mangano, V. Ovchinnikov, D. Bricker, E. Polnau, and A. Rostov, "Deep turbulence effects mitigation with coherent combining of 21 laser beams over 7 km," Opt. Lett. **41**, 840 (2016).
22. T. M. Shay, V. Benham, J. T. Baker, A. D. Sanchez, D. Pilkington, and C. A. Lu, "Self-synchronous and self-referenced coherent beam combination for large optical arrays," IEEE J. Sel. Top. Quantum Electron. **13**, 480 (2007).
23. Y. Ma, X. Wang, J. Leng, H. Xiao, X. Dong, J. Zhu, W. Du, P. Zhou, X. Xu, L. Si, Z. Liu, and Y. Zhao, "Coherent beam combination of 1.08 kW fiber amplifier array using single frequency dithering technique," Opt. Lett. **36**, 951 (2011).
24. Z. Huang, X. Tang, Y. Luo, C. Liu, J. Li, D. Zhang, X. Wang, T. Chen, and M. Han, "Active phase locking of thirty fiber channels using multilevel phase dithering method," Rev. Sci. Instrum. **87**, 033109 (2016).
25. A. Flores, T. Ehrehreich, R. Holten, B. Anderson, and I. Dajani, "Multi-kW coherent combining of fiber lasers seeded with pseudo random phase modulated light," Proc. SPIE **9728**, 97281Y (2016).
26. M. Antier, J. Bourderionnet, C. Larat, E. Lallier, E. Lenormand, J. Primot, and A. Brignon, "kHz closed loop interferometric technique for coherent fiber beam combining," IEEE J. Sel. Top. Quantum Electron. **20**, 182 (2014).
27. I. Fsaifes, L. Daniault, S. Bellanger, M. Veinhard, J. Bourderionnet, C. Larat, E. Lallier, E. Durand, A. Brignon, and J.-C. Chanteloup, "Coherent beam combining of 61 femtosecond fiber amplifiers," Opt. Express **28**, 20152 (2020).
28. R. Liu, C. Peng, X. Liang, and R. Li, "Coherent beam combination far-field measuring method based on amplitude modulation and deep learning," Chin. Opt. Lett. **18**, 041402 (2020).
29. D. Wang, Q. Du, T. Zhou, D. Li, and R. Wilcox, "Stabilization of the 81-channel coherent beam combination using machine learning," Opt. Express **29**, 5694 (2021).
30. F. Li, C. Geng, G. Huang, Y. Yang, X. Li, and Q. Qiu, "Experimental demonstration of coherent combining with tip/tilt control based on adaptive space-to-fiber laser beam coupling," IEEE Photon. J. **9**, 1 (2017).
31. Y. Peng, Q. Hu, J. Duan, D. Li, J. Li, R. Qiao, Z. Shen, Y. Luo, X. Zhao, and D. Zhang, "Active phase locking of laser coherent beam combination using square wave dithering algorithm," J. Russ. Laser Res. **43**, 626 (2022).
32. Y. Yan, Y. Liu, H. Zhang, Y. Li, Y. Li, X. Feng, D. Yan, J. Wang, H. Lin, F. Jing, W. Huang, and R. Tao, "Principle and numerical demonstration of high power all-fiber coherent beam combination based on self-imaging effect in a square core fiber," Photonics Res. **10**, 444 (2022).
33. L. E. Roberts, R. L. Ward, S. P. Francis, P. G. Sibley, R. Fleddermann, A. J. Sutton, C. Smith, D. E. McClelland, and D. A. Shaddock, "High power compatible internally sensed optical phased array," Opt. Express **24**, 13467 (2016).
34. J. Long, H. Chang, Y. Zhang, T. Hou, Q. Chang, R. Su, Y. Ma, P. Ma, and P. Zhou, "Compact internal sensing phase locking system for coherent combining of fiber laser array," Opt. Laser Technol. **148**, 107775 (2022).
35. H. Chang, R. Su, J. Long, Q. Chang, P. Ma, Y. Ma, and P. Zhou, "Distributed active phase-locking of an all-fiber structured laser array by a stochastic parallel gradient descent (SPGD) algorithm," Opt. Express **30**, 1089 (2022).
36. A. Boju, G. Maulion, J. Saucourt, J. Leval, J. Ledortz, A. Koudoro, J.-M. Berthomier, M. Naiim-Habib, P. Armand, V. Kermene, A. Desfarges-Berthelemot, and A. Barthelemy, "Small footprint phase locking system for a large tiled aperture laser array," Opt. Express **29**, 11445 (2021).
37. H. K. Ahn and H. J. Kong, "Cascaded multi-dithering theory for coherent beam combining of multiplexed beam elements," Opt. Express **23**, 12407 (2015).
38. J. Long, R. Su, T. Hou, Q. Chang, M. Jiang, H. Chang, Y. Deng, Y. Ma, P. Ma, and P. Zhou, "System design for coherent combined massive fiber laser array based on cascaded internal phase control," Appl. Opt. **61**, 10222 (2022).
39. A. Lin, H. Zhan, K. Peng, X. Wang, L. Ni, Y. Wang, Y. Li, S. Liu, S. Sun, J. Jiang, X. Tang, Y. Liu, L. Jiang, J. Yu, J. Wang, and F. Jing, "10 kW level pump-gain integrated functional laser fiber," High Power Laser Part. Beams **30**, 060101 (2018).
40. X. Chen, F. Lou, Y. He, M. Wang, Z. Xu, X. Guo, R. Ye, L. Zhang, C. Yu, L. Hu, B. He, and J. Zhou, "Homemade 10 kW fiber laser with high efficiency," Acta Opt. Sin. **39**, 0336001 (2019).